Lattice model for surfactants in solution

M. W. Matsen and D. E. Sullivan
Department of Physics and Guelph-Waterloo Program for Graduate Work in Physics, University of Guelph, Guelph, Ontario, Canada N1G 2W1
(Received 2 August 1989; revised manuscript received 17 October 1989)

A three-dimensional lattice model for surfactant mixtures is presented in this paper. We extend the spin-1 or Blume-Emery-Griffiths model to include orientational degrees of freedom for each molecule. The model is then applied to ternary mixtures of surfactant with equal amounts of water and oil, and to binary mixtures of surfactant and water. For each case, phase diagrams are calculated using both mean-field and Bethe approximations. One interesting feature of this model is that it can exhibit long-period lamellar phases even though a simple Hamiltonian, containing only nearest-neighbor interactions, is used. The model also produces a "disorder line," which is thought to divide the disordered phase of the ternary mixture into a region of ordinary disordered fluid and a region of microemulsion.

I. INTRODUCTION

Liquid mixtures of water, oil, and surfactant (amphiphile) exist in numerous phases, which are of both commercial and biological interest. The underlying reason for the rich behavior of these mixtures is due to the tendency of the surfactant molecules to position themselves along water-oil interfaces. Recently, a substantial effort has gone into finding models which reproduce the phases observed experimentally.[1-17] A new model, which exhibits some of these phases, is introduced in this paper.

For a liquid mixture of water and oil there are three possible isotropic phases. At high temperatures, the water and oil molecules mix in a disordered phase, but at lower temperatures, the water and oil separate into water-rich and oil-rich phases, resulting in a water-oil interface. Away from the critical point, the surface tension of such an interface is quite large, about 50 dyn/cm. The addition of surfactant molecules often decreases this surface tension by several orders of magnitude, causing the water and oil regions to mix down to microscopic scales.

A typical surfactant molecule consists of a polar head group with a hydrocarbon tail attached to it. The polar head group is more attracted to water than to oil, and vice versa for the hydrocarbon tail, making it favorable for a surfactant molecule to be located between water and oil molecules. It is this mechanism which tends to mix the water and oil molecules, competing against their natural tendency to separate. This results in numerous phases such as the microemulsion, lamellar, hexagonal, and cubic phases. A brief discussion of these different phases can be found in the paper by Chen *et al.*[4]

One approach to studying these mixtures is to use phenomenological models.[1-3] An advantage of such an approach is the ability to model features that are difficult to treat in a molecular theory. A disadvantage is that the free energy depends upon coefficients whose relation to molecular properties is unspecified. Furthermore, relevant types of microstructures, such as bilayer membranes, are assumed to exist *a priori* rather than being derived through a statistical treatment of molecular association.

Recently, several molecular models of surfactant solutions have been examined. Most of these models employ a discrete translational phase space,[4-14] where the volume of the fluid is divided into a lattice of cubical molecular-sized cells. At each lattice site is placed one of the three types of molecules. As one may notice, the lattice forces the spacing between all molecules to be equal, and consequently each molecule has the same effective volume. In reality, the size of a water or oil molecule is smaller than a surfactant molecule. This can be ignored if all one desires is a model which reproduces qualitatively the phases of the real system, since varying sizes of the molecules is not responsible for the existence of the different phases. Alternatively, a site occupied by water could be assumed to contain a number of molecules such that their volume equals the volume of one surfactant molecule.[5] The same would apply to sites occupied by oil.

The restriction of the lattice site occupancy removes the need to consider the hard-core part of the intermolecular potentials, leaving only the attractive portion to consider. For each pair of molecules, the intermolecular potential depends both on their separation and relative orientations. Most of the models have ignored the orientational dependence of the water and oil molecules. The orientations of the surfactant molecules cannot be ignored, as there is an important distinction between the head and tail of such a molecule. Schick and coworkers[6-8] and Chen *et al.*[4] have constructed models where the orientation of surfactant molecules is not specified, and have instead used three-particle interactions which favor having a water and oil molecule on opposite sides of a surfactant molecule to mimic the behavior of the surfactant. The model considered by Widom and co-workers[9-11] does account for surfactant orientations, although at present the identification of microemulsion phases in that model is problematic.[10] A summary and critique of the above theories have been

given by Gompper and Schick.[12]

The model examined in this paper is similar to ones recently considered in Refs. 5, 13, and 14. All of these models explicitly allow for surfactant orientational degrees of freedom. The main differences between the models are due to the forms of the intermolecular potentials used, those in the present paper being rather more general than in previous works (as noted in Sec. II). As in the work by Ciach, Høye, and Stell,[13] the present model allows for only discrete orientations of the molecules, so that the polar head group of a surfactant can only point toward one of its six nearest neighbors. At the level of approximations and for the types of phases considered, we do not expect that the results would be qualitatively modified on allowing for continuous orientations.[5,14]

We note that there have been some attempts to study models that retain a continuous translational phase space. This has been done by Ciach, Høye, and Stell[13] for a one-dimensional model, while retaining a discrete orientational phase space. A model which is fully continuous in both positions and orientations has been used by Telo da Gama and Gubbins[15] to examine the interface between water-rich and oil-rich phases. Another such model for water-surfactant mixtures has been studied using molecular-dynamics methods by Gunn and Dawson.[16]

An advantage of using a discrete model over a continuous model is the increased number of methods that can be used to calculate the free energy. With continuous models in three dimensions, one is realistically forced to use mean-field theory, a single-particle cluster method. With lattice models one can also use larger cluster methods, renormalization-group methods, temperature series expansions, as well as several other methods. In this paper, both the mean-field and Bethe (or two-particle cluster) methods are used. Our results for the temperature-dependent phase diagrams are considerably more extensive than those described in Refs. 5, 13, and 14.

There is a similar interest in binary mixtures of water and surfactant.[5,14] In these mixtures, the surfactant molecules try to arrange themselves as to only expose their polar head groups to the water molecules. Just as for the ternary mixtures, these mixtures exhibit a variety of phases such as the lamellar, hexagonal, cubic, and micellar phases. The model chosen in this paper treats the interactions in a sufficiently realistic way that it can be applied to these binary mixtures.

II. MODEL

To model this three-component system, an extension of the spin-1 or Blume-Emery-Griffiths (BEG) model[18] on a cubic lattice is used. The vector $\mathbf{r}_{ij}$, measured in units of the lattice spacing, is used to specify the direction from lattice site i to lattice site j. As in the spin-1 or BEG model, at each lattice site i there is a statistical variable σ_i which can take on the values $+1$, 0, or -1, which in this case represent water, surfactant, or oil, respectively. The extension to the spin-1 model is a second statistical variable $\mathbf{s}_i$ at each site specifying the orientation of the molecule. In general, one could allow the orientations to vary continuously, although in this paper we shall restrict $\mathbf{s}_i$ to point only toward one of the six nearest neighbors (NN) of site i. For a surfactant molecule, $\mathbf{s}_i$ represents the direction of the polar head group.

For simplicity, the Hamiltonian is chosen so that the energy of the system is independent of the orientation of the water and oil molecules. Hence for the water and oil, the orientational degrees of freedom due to $\mathbf{s}_i$ contribute just to the entropy and not to the energy. For additional simplicity, the Hamiltonian is chosen to contain only NN pair interactions, and to treat symmetrically the water and oil molecules and the two ends of the surfactant molecules. With these symmetries, the most general Hamiltonian is

$$H=-\sum_{\langle ij\rangle}\sum_{\alpha=1}^{4}(J_\alpha P_{\alpha,ij}+K_\alpha P_{\alpha,ij}^2)-\mu_s\sum_i \rho_i \ , \tag{1}$$

where

$$\rho_i=1-\sigma_i^2 \ , \tag{1a}$$

$$P_{1,ij}=\sigma_i\sigma_j \ , \tag{1b}$$

$$P_{2,ij}=\sigma_i(\rho_j\mathbf{s}_j\cdot\mathbf{r}_{ji})+\sigma_j(\rho_i\mathbf{s}_i\cdot\mathbf{r}_{ij}) \ , \tag{1c}$$

$$P_{3,ij}=(\rho_i\mathbf{s}_i\cdot\mathbf{r}_{ij})(\rho_j\mathbf{s}_j\cdot\mathbf{r}_{ji}) \ , \tag{1d}$$

$$P_{4,ij}=-(\rho_i\mathbf{s}_i\times\mathbf{r}_{ij})\cdot(\rho_j\mathbf{s}_j\times\mathbf{r}_{ji}) \ . \tag{1e}$$

The symbol $\langle ij\rangle$ denotes that the summation is over all distinct pairs of NN sites i and j. The constants J_α and K_α for $\alpha=1-4$ determine the bonding energies, and μ_s is the surfactant chemical potential to within an additive constant.

Notice that all the terms in the Hamiltonian, the $P_{\alpha,ij}$'s and the ρ_i's, are invariant under any even number of the following transformations. T_1: $\sigma_i \Longrightarrow -\sigma_i$, which interchanges all water and oil molecules; T_2: $\mathbf{s}_i \Longrightarrow -\mathbf{s}_i$, which flips all surfactant molecules; and T_3: $\mathbf{r}_{ij} \Longrightarrow -\mathbf{r}_{ij}$, which inverts the lattice. In Table I, these transformations are applied to a single representative bond between two NN lattice sites, demonstrating that the energy of a bond remains unchanged after an even number of transformations. It specifically shows that the bonds $\rightarrow\circ$ and $\leftarrow\bullet$ have the same energy, and similarly, the bonds $\rightarrow\bullet$ and $\leftarrow\circ$ have equal energies. (An open circle represents a water molecule, a solid circle represents an oil molecule, and an arrow represents a surfactant molecule and its orientation $\mathbf{s}_i$.)

Due to these symmetries, only 11 of all the possible bonds between NN sites are distinct. That is, any bond

TABLE I. Symmetry transformations applied to a single bond.

Transformation	Bond	Energy
Initial bond	$\rightarrow\circ$	$-J_2-K_2$
T_1	$\rightarrow\bullet$	J_2-K_2
T_2	$\leftarrow\bullet$	$-J_2-K_2$
T_3	$\bullet\leftarrow$	J_2-K_2
T_1	$\circ\leftarrow$	$-J_2-K_2$
T_2	$\circ\rightarrow$	J_2-K_2

can be obtained by some even number of transformations on one of the 11 distinct bonds. These 11 bonds are shown in Table II. Under the condition of water-oil symmetry, the Hamiltonian is completely general, even though the energy for three of the distinct bonds is chosen to be zero. It is possible to do this because of the chemical-potential term in the Hamiltonian, and the constraints that all lattice sites must be occupied and that all surfactant molecules must point to one of their nearest neighbors.

To give this model the proper behavior for the ternary mixture, the J_α's are chosen to be positive. The K_α's are less crucial to the phase diagram, and for this paper have been chosen to be zero. A positive J_1 favors oil-water separation, and a positive J_2 gives the surfactant tails their hydrophobic behavior and the heads their hydrophilic behavior. When J_3 is positive, the surfactant molecules tend to line up tail to tail or head to head, as opposed to tail to head. Finally, a positive J_4 favors the alignment of surfactant molecules parallel rather than antiparallel when side by side. The results that are presented later have been obtained using the following ratio of the bonding energies:

$$J_1=J_2=\tfrac{4}{3}J_3=\tfrac{4}{5}J_4\equiv J>0\ , \tag{2a}$$

$$K_1=K_2=K_3=K_4=0\ . \tag{2b}$$

As noted previously, the lattice models in Refs. 5, 13, and 14 are similar to the present model in that they explicitly include orientational degrees of freedom for the molecules. The model in Ref. 13 is applied to water-oil-surfactant mixtures and those in Refs. 5 and 14 are applied to water-surfactant mixtures, while the present model is applied to both. The Halley-Kolan model[5] and the Dawson-Kurtovic model[14] allow for continuous rather than discrete orientations. All three models are less general in their treatment of surfactant-surfactant interactions than the present model. Dawson and Kurtovic[14] include an interaction disfavoring orthogonal alignment between NN surfactant molecules, but independent of the lattice vectors $\mathbf{r}_{ij}$ and (in the particular case studied) not distinguishing between surfactant head and tail. The model of Ref. 5 does not include any orientation-dependent surfactant-surfactant interactions, while Ciach and co-workers[13] consider only a very simplified, two-state representation of these interactions. Apart from asymptotic results at low temperatures and near critical points, global phase diagrams for the models in Refs. 13 and 14 have not been calculated, while these are investigated for the present model in the following sections.

TABLE II. The distinct bonds. ⊙ denotes an arrow directed out of the page.

Bond	Energy	Bond	Energy
○○	$-J_1-K_1$	↑↑	$-J_4-K_4$
○●	J_1-K_1	↑↓	J_4-K_4
→○	$-J_2-K_2$	○↑	0
→●	J_2-K_2	→↑	0
→←	$-J_3-K_3$	⊙↑	0
→→	J_3-K_3		

III. MEAN-FIELD AND BETHE APPROXIMATIONS

In this section, a method is described for calculating, in either the mean-field or Bethe approximation, the free energy associated with the more general Hamiltonian

$$H=\sum_{(ij)}V_{ij}(x_i,x_j)+\sum_i V_i(x_i)\ . \tag{3}$$

The symbol (ij) on the first summation denotes that the sum is carried out over all distinct pairs of lattice sites. The x_i's are the state variables, the $V_i(x_i)$'s are the one-particle potentials, and the $V_{ij}(x_i,x_j)$'s are the two-particle potentials. For the specific Hamiltonian used in this paper,

$$x_i=\{\sigma_i,\mathbf{s}_i\}\ , \tag{4a}$$

$$V_i(x_i)=-\mu_s\rho_i\ , \tag{4b}$$

$$V_{ij}(x_i,x_j)=\begin{cases}-\sum_{\alpha=1}^{4}(J_\alpha P_{\alpha,ij}+K_\alpha P_{\alpha,ij}^2), & \text{if } i \text{ and } j \text{ are NN}\\ 0, \quad \text{otherwise}\ .\end{cases} \tag{4c}$$

The mean-field and Bethe approximations require one to solve for one-particle and two-particle distribution functions, respectively. The single-particle distribution function $p_i(x_i)$ gives the probability that site i is in the state x_i. These probability distribution functions must satisfy the normalization condition

$$\sum_{x_i}p_i(x_i)=1\ . \tag{5}$$

Similarly, the two-site probability distribution function $p_{ij}(x_i,x_j)$ gives the probability that site i is in state x_i and site j is in state x_j. These probability distribution functions must satisfy

$$\sum_{x_j}p_{ij}(x_i,x_j)=p_i(x_i)\ . \tag{6}$$

With this method, one isolates a cluster of sites using effective fields to replace the interactions of the cluster with the remaining system. $U_{ij}(x_i)$ is defined to be the effective field acting on site i due to a different site j, when site i is in the state x_i. To begin, the energy of a single-particle cluster at site i is

$$E_i(x_i)=V_i(x_i)+\sum_{j\neq i}U_{ij}(x_i) \tag{7}$$

and

$$p_i(x_i)=c_i\exp[-\beta E_i(x_i)]\ , \tag{8}$$

where $\beta\equiv(k_BT)^{-1}$ is the inverse temperature and the constant c_i is determined by Eq. (5). In the mean-field approximation, one stops here with the effective fields given by

$$U_{ij}(x_i)=\sum_{x_j} p_j(x_j)V_{ij}(x_i,x_j) \ . \tag{9}$$

The energy of a two-particle cluster is

$$E_{ij}(x_i,x_j)=V_i(x_i)+V_j(x_j)+V_{ij}(x_i,x_j) + \sum_{k\neq i,j}[U_{ik}(x_i)+U_{jk}(x_j)] \tag{10}$$

and

$$p_{ij}(x_i,x_j)=c_ic_j\exp[-\beta E_{ij}(x_i,x_j)] \ . \tag{11}$$

Choosing c_ic_j as the constant in Eq. (11), although convenient, was arbitrary. In the Bethe approximation, the $U_{ij}(x_i)$'s are determined by requiring Eq. (6) to be satisfied. Substituting Eqs. (7), (8), (10), and (11) into (6) gives

$$\exp[-\beta U_{ij}(x_i)] =c_j\sum_{x_j}\exp\left[-\beta\left[V_j(x_j)+V_{ij}(x_i,x_j) + \sum_{k\neq i,j}U_{jk}(x_j)\right]\right] \tag{12}$$

Note that if $V_{ij}(x_i,x_j)=0$ for all x_j, then $U_{ij}(x_i)=0$. Therefore, for a Hamiltonian with only NN interactions, $U_{ij}(x_i)$ is zero if i and j are not NN sites.

For either of the two approximations, one can now create a system of equations where the only unknowns are the effective fields. For the mean-field approximation, using Eqs. (5), (7), and (8), one expresses $p_j(x_j)$ in terms of the effective fields and substitutes the result into (9). Similarly for the Bethe approximation, using Eqs. (5), (7), and (8), one expresses c_j in terms of the effective fields and substitutes that result into (12), to obtain the system of equations.

One can now solve the system of equations for either approximation to find the effective fields. Usually for a given location on the phase diagram, there are multiple solutions, each corresponding to a different phase. When a number of solutions exist simultaneously, the physically accepted solution will be that which minimizes the free energy. In some cases, there can even be an infinite number of solutions, and consequently a certain degree of judgment is required to retain only the reasonable phases to be solved for. We believe that for our model, we have considered all the reasonable phases, and therefore believe that our phase diagrams are complete.

For all the phases that we had to consider, there were only a finite number of distinct effective fields (the number varied from 3 to about 50). Thus these systems of equations were of reasonable size and could be solved by the Newton-Raphson iteration method. For a trial solution from which to start the iterations, it is generally sufficient to use the $T=0$ solution for an ordered phase or the $T=\infty$ solution for a disordered phase, both being solutions that can be obtained analytically.

Having solved for the effective fields, one needs to evaluate the free energy corresponding to each solution to determine which are physically acceptable. First, one calculates c_i and $p_i(x_i)$ using Eqs. (5), (7), and (8). In the mean-field approximation $p_{ij}(x_i,x_j)=p_i(x_i)p_j(x_j)$, while in the Bethe approximation it is given by Eqs. (10) and (11). Once the probability distribution functions are known, the free energy can be obtained from

$$F=E-TS \ , \tag{13}$$

where

$$E=\sum_i\sum_{x_i}p_i(x_i)V_i(x_i) +\sum_{(ij)}\sum_{x_i,x_j}p_{ij}(x_i,x_j)V_{ij}(x_i,x_j) \ , \tag{13a}$$

$$S=-k_B\sum_i\sum_{x_i}p_i(x_i)\ln[p_i(x_i)] -k_B\sum_{(ij)}\sum_{x_i,x_j}\{p_{ij}(x_i,x_j)\ln[p_{ij}(x_i,x_j)] -p_i(x_i)p_j(x_j)\ln[p_i(x_i)p_j(x_j)]\} \ . \tag{13b}$$

Equation (13a) is the definition of average energy, and thus is exact. The entropy given by Eq. (13b) is an approximation, which comes from a series expansion in n-site probability distribution functions truncated at $n=2$.[19] Fortunately, due to the choice of c_ic_j as the constant in Eq. (11), the free energy according to Eq. (13) is also given by simpler expressions, (14a) for the mean-field approximation and (14b) for the Bethe approximation:

$$F_{\rm MF}=k_BT\sum_i\ln(c_i)-\sum_{(ij)}\sum_{x_i,x_j}p_i(x_i)p_j(x_j)V_{ij}(x_i,x_j) \ , \tag{14a}$$

$$F_B=k_BT\sum_i\ln(c_i) \ . \tag{14b}$$

An equivalent method for the mean-field approximation is to substitute $p_{ij}(x_i,x_j)=p_i(x_i)p_j(x_j)$ into (13), and to minimize the free energy with respect to the $p_i(x_i)$'s, under the constraint of Eq. (5). Similarly, there is a variational method equivalent to the Bethe approximation. In this case, one minimizes Eq. (13) with respect to the $p_{ij}(x_i,x_j)$'s, under the constraints of Eqs. (5) and (6). Ng and Barry describe this method in detail for the BEG model.[20]

IV. PHASE DIAGRAM FOR THE TERNARY MIXTURE

With the choice of bonding energies made previously, we find six phases, five of which are ordered phases. Two of the ordered phases are uniform and the other three are nonuniform layered phases. These ordered phases generally exist at low temperatures. At high temperatures, there is a disordered phase (D), for which the entropy is large and the occupation of lattice sites is more or less random.

The water-rich phase (W) and oil-rich phase (O) are the two uniform ordered phases. Because of the symmetry between water and oil in the Hamiltonian, the W and

O phases both have the same free energy, and consequently are always in coexistence. The free energy per lattice site to first order in temperature is

$$F_{W+O} \simeq -3(J_1+K_1)-k_BT\ln(6) . \quad (15)$$

The entropy $k_B\ln(6)$ is due to the orientational degeneracy of the water and oil molecules.

This model also exhibits a number of lamellar phases (L_n), where there are surfactant monolayers separated alternately by n layers of water and n layers of oil. At low temperatures, the free energy per site for these phases is approximately

$$F_{Ln} \simeq E_{\text{wall}}/(n+1)+F_{W+O} , \quad (16)$$

where the domain-wall free energy[6] is given by

$$E_{\text{wall}}=4(J_1+K_1)-2(J_2+K_2)-2(J_4+K_4) +k_BT\ln(6)-\mu_s . \quad (16')$$

At nonzero temperatures, our numerical results indicate that there is always a finite number of lamellar phases, where the number depends on the choice of bonding energies. For the choice made previously [Eq. (2)], there are just the two lamellar phases L_1 and L_2.[21] It seems possible that for this model, lamellar phases which do not have the simple periodic layering described above could also exist, although such phases never seem to be energetically favorable except at $T=0$.

The last ordered phase is the surfactant-rich phase (S). This phase consists of layers of surfactant, arranged so that the polar heads of one layer are adjacent to the polar heads of a neighboring layer, and similarly for the hydrocarbon tails. Most models to date have not exhibited an equivalent phase, as a consequence of not including orientational interactions between the surfactant molecules. (The Dawson and Kurtovic[14] model, used for water-surfactant mixtures, is one exception.) The free energy per site for this phase at low temperatures is approximately

$$F_S \simeq -(J_3+K_3)-2(J_4+K_4)-\mu_s . \quad (17)$$

Figure 1 is a schematic diagram of each of the five ordered phases at zero temperature.

Following are the phase diagrams calculated by both the mean-field approximation (Figs. 2 and 3) and Bethe approximation (Figs. 4 and 5). In each case, the phase diagram is plotted in both the temperature and surfactant-chemical-potential plane, and the temperature and mean-surfactant-density plane, where the latter is denoted ρ_s. The solid lines represent first-order transitions, and the dashed lines represent second-order transitions. The dotted lines represent the "disorder line," which will be discussed later.

In the chemical-potential plots, the L_2 phase is an extremely narrow strip between the $W+O$ and L_1 phases, from $T=0$ to the first dot marking the multiphase point where W, O, L_1, and L_2 coexist (1). Also marked by dots are the multiphase points where W, O, L_1, and D coexist (2), and where L_1, D, and S coexist (3). [In Fig. 2 for the mean-field approximation, the points (1) and (2) are indistinguishable on the scale of the diagram.] The tricritical point where the first-order line between $W+O$ and D turns into a second-order line is also marked by a dot (4). Also of interest are the limiting temperatures for the second-order line as $\mu_s \to -\infty$ (5), and for the first-order line between S and D as $\mu_s \to +\infty$ (6). These six points are given in Table III.

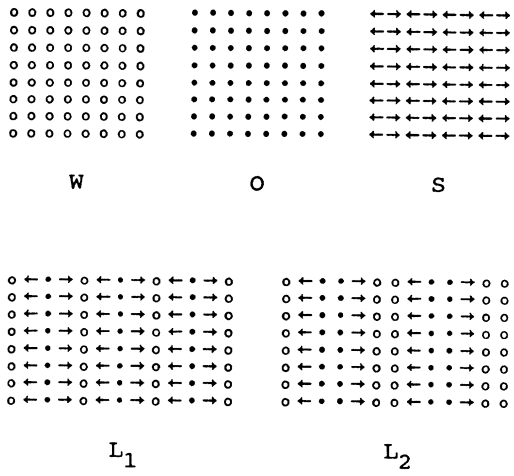

FIG. 1. Schematic diagrams of the five ordered phases of the ternary mixture at $T=0$.

At low temperatures, the line which separates $W+O$ and L_1 and on which all the lamellar phases L_n ($n>1$) exist is approximately given by $E_{\text{wall}}=0$

$$\mu_s \simeq k_BT\ln(6)+4(J_1+K_1)-2(J_2+K_2)-2(J_4+K_4) . \quad (18)$$

The first-order line between L_1 and S is found by solving $F_{L_1}=F_S$. Using Eqs. (16) and (17), it follows that at low temperatures, this line is given by

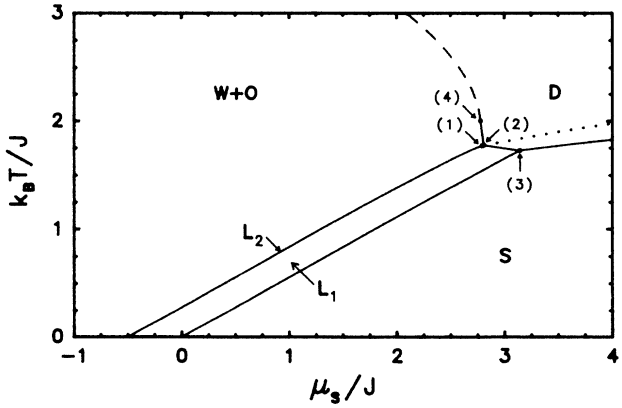

FIG. 2. Phase diagram of the ternary mixture calculated by the mean-field approximation and plotted in the temperature and surfactant-chemical-potential plane. The solid lines denote first-order transitions, and the dashed line denotes a second-order transition.

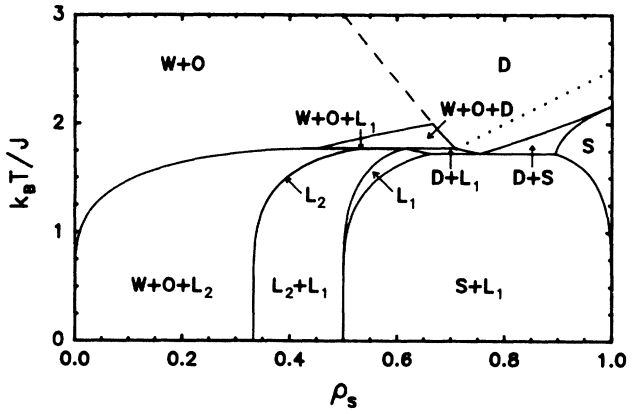

FIG. 3. Phase diagram of the ternary mixture calculated by the mean-field approximation and plotted in the temperature and surfactant-density plane. The solid lines denote first-order transitions, and the dashed line denotes a second-order transition. The disorder line is shown with a dotted line.

$$\mu_s \simeq k_B T \ln(6) + 2(J_1 + K_1) + 2(J_2 + K_2) - 2(J_3 + K_3) - 2(J_4 + K_4) . \quad (19)$$

From Eqs. (18) and (19), the approximate width of the L_1 phase Δ_{L_1} along the μ_s axis is

$$\Delta_{L_1} \simeq -2(J_1 + K_1) + 4(J_2 + K_2) - 2(J_3 + K_3) . \quad (20)$$

In order that the lamellar phases exist in the phase diagram, one must choose the above width to be positive. Figures 2 and 4 show that the low-temperature asymptotic result (20) is indeed closely obeyed over most of the region in which the lamellar phase L_1 exists.

The mean-field results compare reasonably well to those obtained by the presumably more accurate Bethe approximation. The locations of features in the phase diagram are noticeably different for the two methods, but nevertheless they both predict the same features in relatively the same locations. Thus if all one wanted were topologically correct phase diagrams, then the mean-field approximation should be sufficient.

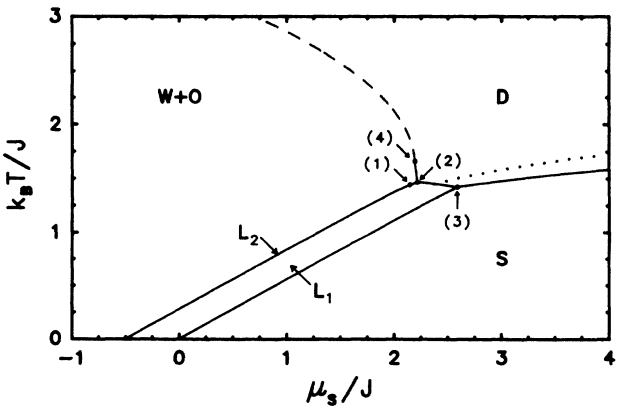

FIG. 4. Same diagram as in Fig. 2, but obtained by the Bethe approximation.

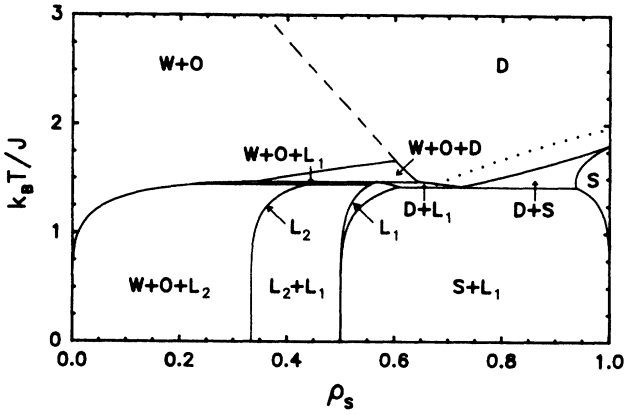

FIG. 5. Same diagram as in Fig. 3, but obtained by the Bethe approximation.

V. DISORDER LINE

An isotropic phase of the water-oil-surfactant mixtures which has received must interest is the microemulsion phase.[1-4,6-13] At small oil concentrations, this phase is believed to consist of small droplets of oil separated from the surrounding water by surfactant layers. When the water concentration is small, there are small droplets of water surrounded by surfactant in oil. When the water and oil concentrations are comparable as in the present model, the water and oil regions are rather complex bicontinuous structures where surfactant collects along the vast water-oil interface.[4] In lattice models, it is the general consensus that the microemulsion corresponds to the disordered phase or at least a portion of this phase.[4,8,10,12]

An experimental signature of a microemulsion is the existence of a maximum in the water-water structure factor at a small nonzero value of the wave number $q_{\max}$.[8,10,12,22] Gompper and Schick[8,12] have proposed that a convenient theoretical boundary between microemulsion and "ordinary" disordered fluid is the line at which $q_{\max}(\mu_s, T) \to 0$. This does not represent a real phase boundary, as one expects the free energy to be analytic on crossing this line. Here we locate this boundary by calculating the structure factor generated by the present model, that is, we evaluate the Fourier transform of the water-water correlation function. Generally, the correlation functions are defined in terms of the one-site

TABLE III. Coordinates of six points along phase boundaries in the phase diagram for the ternary mixture.

Point	Mean-field approximation μ_s/J	k_BT/J	Bethe approximation μ_s/J	k_BT/J
1	2.7903	1.7704	2.1439	1.4411
2	2.8048	1.7748	2.2128	1.4664
3	3.1376	1.7250	2.5873	1.4190
4	2.7726	2.0	2.1908	1.6635
5	$-\infty$	6.0	$-\infty$	4.9326
6	$+\infty$	2.1667	$+\infty$	1.8073

and two-site probability distribution functions

$$\hat{p}_{ij}(x,x') \equiv p_{ij}(x,x')(1-\delta_{ij}) - p_i(x)p_j(x') + p_i(x)\delta_{ij}\delta_{x,x'} , \tag{21}$$

where $x=\{\sigma,\mathbf{s}\}$ denotes the state of a lattice site. (The water-water correlation function corresponds to the case $\sigma=\sigma'=1$.) Note that if the two-site probabilities $p_{ij}(x,x')$ described in Sec. III are used in (21), the resulting correlation function $\hat{p}_{ij}(x,x')$ is strictly of finite range in both mean-field and Bethe approximations, and thus does not exhibit the characteristic long-range structure of interest. Therefore, we calculate $\hat{p}_{ij}(x,x')$ by an alternate method, equivalent to an Ornstein-Zernike approximation, as was done in Refs. 8 and 10.

The most straightforward way of obtaining $\hat{p}_{ij}(x,x')$ is based on the exact functional relation

$$\hat{p}_{ij}(x,x') = -k_B T \frac{\delta p_i(x)}{\delta V_j(x')} , \tag{22}$$

that is, considering the response of $p_i(x)$ to small variations in the one-particle potentials $V_j(x')$. Applying (22) to the self-consistent relations for the one-site probabilities described in Sec. III yields an equation for $\hat{p}_{ij}(x,x')$ of Ornstein-Zernike form,

$$\hat{p}_{ij}(x,x') = \hat{p}^{(0)}_{ij}(x,x') + \sum_{k,y}\sum_{l,z} \hat{p}^{(0)}_{ik}(x,y)c_{kl}(y,z)\hat{p}_{lj}(z,x') , \tag{23}$$

where

$$\hat{p}^{(0)}_{ij}(x,x') \equiv p_i(x)[\delta_{x,x'} - p_j(x')]\delta_{ij} \tag{23'}$$

is the ideal-lattice-gas correlation function. In the mean-field case, the "direct correlation function" $c_{ij}(x,x')$ is given by the expected form

$$c_{ij}(x,x') = -\beta V_{ij}(x,x')(1-\delta_{ij}) . \tag{24}$$

The direct correlation function generated by the Bethe approximation, not shown here, is more complicated, due to the more elaborate self-consistency involved in that approximation, although as in (24) it is still found to vanish for lattice separations greater than the NN distance.

A Fourier transformation conveniently simplifies Eq. (23) for the translational-invariant disordered phase, where the one-site probability is independent of both the site position and the orientational variable s. Denoting the Fourier transform of $\hat{p}_{ij}(x,x')$ by $\hat{p}_q(x,x')$, where q is the wave vector, the resulting matrix equation for $\hat{p}_q(x,x')$ in the finite x-variable space is straightforwardly solved. In particular, we obtain the water-water structure factor $S_{w\text{-}w}(\mathbf{q}) \propto \hat{p}_q(x,x')$ for $\sigma=\sigma'=1$. The dotted lines in the phase diagrams of Figs. 2–5 represent the loci where the $q_{\max}$ displayed by this structure factor vanishes continuously. In each diagram, the microemulsion characterized by nonzero $q_{\max}$ exists to the right (at higher μ_s or ρ_s) of the dotted line. We shall call the latter the "disorder line,"[23] although this term really refers to a somewhat less restrictive and less experimentally useful criterion for the existence of a microemulsion.[8,12]

Expanding the structure factor for small $q \equiv |\mathbf{q}|$ as

$$S_{w\text{-}w}(\mathbf{q}) = S_{w\text{-}w} + Bq^2 + O(q^4) \tag{25}$$

the disorder line corresponds to the locus where $B=0$. We note that the water-water structure factor when expanded to order q^2 is independent of q's orientation, even though the model uses a lattice which is not invariant under arbitrary rotations. In the mean-field approximation, the disorder line is found to be given by (for parameters $K_\alpha=0$)

$$\frac{k_B T}{J_1} = \frac{2}{3}\left[2\left[\frac{J_2}{J_1}\right]^2 - \frac{J_3}{J_1} + 2\frac{J_4}{J_1}\right]\rho_s . \tag{26}$$

For the parameter values used here [Eq. (2)], this becomes

$$\frac{k_B T}{J} = \tfrac{5}{2}\rho_s . \tag{26'}$$

A simple analytical expression for the disorder line in the Bethe approximation has not been obtained, although its behavior is found by numerical methods to be similar to that of (26). As seen in Figs. 2–5, in both approximations the disorder line lies just above the first-order lines separating the disordered phase from the lamellar and surfactant-rich phases. By our criterion, the microemulsion exists only in the narrow strip between these first-order lines and the disorder line. In particular, the microemulsion does not exist up to arbitrarily high temperatures. This behavior contrasts with that found in Ref. 8, which implies that the structured disordered fluid (with $q_{\max}\neq 0$) is maintained at all temperatures. The latter feature reflects the fact that the amphiphilic interactions in Ref. 8 are associated with a temperature-independent three-particle potential. In practice, such an effective interaction should be temperature-dependent due to entropic effects associated with the underlying orientational degrees of freedom.

The proximity of the disorder line to the phase boundary between disordered and layered phases is not accidental. By a Landau expansion of the free energy,[2,6] it can be shown that the locus $q_{\max}\to 0$ coincides with a necessary, though generally insufficient, condition for stability of an ordered phase characterized by a nonzero wave vector. This connection between microemulsions and the ordered lyotropic phases provides quantitative support for arguments discussed in Ref. 12.

In Figs. 2–5, the disorder line intersects the first-order boundary between disordered and lamellar (L_1) phases. Thus, with the present choice of microscopic parameters, there is no region where the microemulsion coexists with the uniform water-rich and oil-rich phases, contrary to the usual experimental situation. However, (26a) indicates that a slight change in model parameters will shift the disorder line to higher temperatures and may possibly result in water-oil-microemulsion coexistence. We note also that the region of the disordered phase to the right of the disorder line does not extend below about 68 vol% surfactant concentration, whereas in real microemulsions the surfactant concentration can be as low as a few percent (by volume). A similar unphysical result was found

in Ref. 4, where it was pointed out that some mitigation could be achieved by a rescaling of the concentrations to reflect different sizes of the surfactant and water molecules (see Sec. I).

VI. PHASE DIAGRAM FOR THE BINARY MIXTURE

Repeating the calculations done for the ternary mixture, but restricting σ_i to only take on the values 0 or 1, gives results for a binary mixture of water and surfactant. The results for this mixture are similar to those for the ternary mixture, but this binary mixture exhibits only four phases.

What was previously the water-rich phase and the disordered phase has now become one phase denoted by D. This phase changes continuously from a phase of high water concentration at low temperatures to a phase similar to the previous disordered phase at high temperatures.[24] The free energy per site to first order in temperature is

$$F_D \simeq -3(J_1+K_1)-k_BT\ln(6)\ . \tag{27}$$

Again, for the present choice of bonding energies, we find that there are only two lamellar phases L_1 and L_2. For this binary mixture the phase L_n consists of surfactant bilayers separated by n layers of water. At low temperatures, the free energy per site is approximately

$$F_{L_n} \simeq E_{\text{wall}}/(n+2)+F_{W+O}\ , \tag{28}$$

where

$$E_{\text{wall}}=7(J_1+K_1)-2(J_2+K_2)-(J_3+K_3) -4(J_4+K_4)+2k_BT\ln(6)-2\mu_s\ . \tag{28'}$$

Schematic diagrams of the two new lamellar phases at $T=0$ are shown in Fig. 6.

As for the ternary mixture, the binary mixture has a nonuniform surfactant-rich phase (S), due to orientational interactions between the surfactant molecules. Again at low temperatures, the free energy per site is approximately

$$F_S \simeq -(J_3+K_3)-2(J_4+K_4)-\mu_s\ . \tag{29}$$

For the two approximations to the chemical-potential phase diagram (Figs. 7 and 9) for the binary mixtures, the L_2 phase is an extremely narrow region between the D and L_1 phases, from $T=0$ to the first dot at the multi-

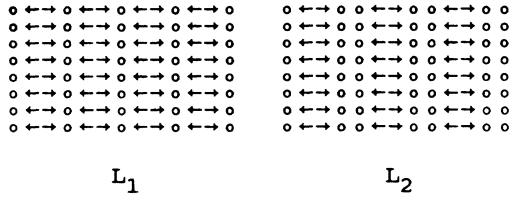

FIG. 6. Schematic diagrams of the two lamellar phases of the binary mixture at $T=0$.

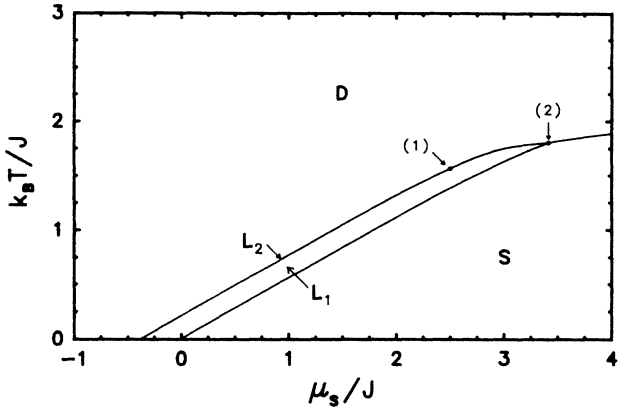

FIG. 7. Phase diagram of the binary mixture calculated by the mean-field approximation and plotted in the temperature and surfactant-chemical-potential plane. All lines denote first-order transitions.

phase point where D, L_1, and L_2 coexist (1). Also marked by a dot is the multiphase point where D, L_1, and S coexist (2). One other point of interest is the limiting temperature for the first-order line between S and D as $\mu_s \to +\infty$ (3). The locations of these three points are given in Table IV.

The narrow L_2 region in the chemical-potential phase diagram, which separates D and L_1 at low temperatures, is approximately given by the line $E_{\text{wall}}=0$,

$$\mu_s \simeq k_BT\ln(6)+\tfrac{7}{2}(J_1+K_1)-(J_2+K_2) -\tfrac{1}{2}(J_3+K_3)-2(J_4+K_4)\ . \tag{30}$$

The line separating L_1 and S is found by solving $F_{L_1}=F_S$, which at low temperatures is approximately

$$\mu_s \simeq k_BT\ln(6)+2(J_1+K_1)+2(J_2+K_2) -2(J_3+K_3)-2(J_4+K_4)\ . \tag{31}$$

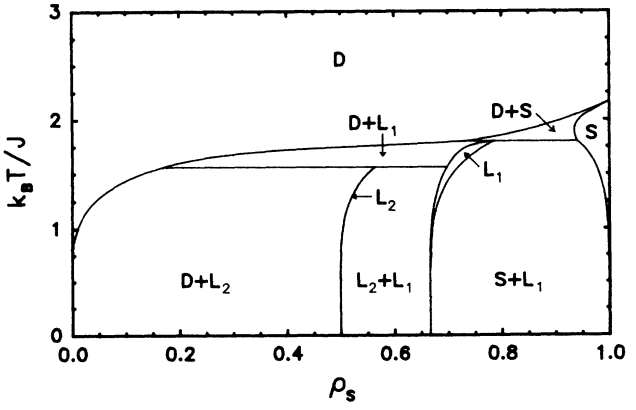

FIG. 8. Phase diagram of the binary mixture calculated by the mean-field approximation and plotted in the temperature and surfactant-density plane. All lines denote first-order transitions.

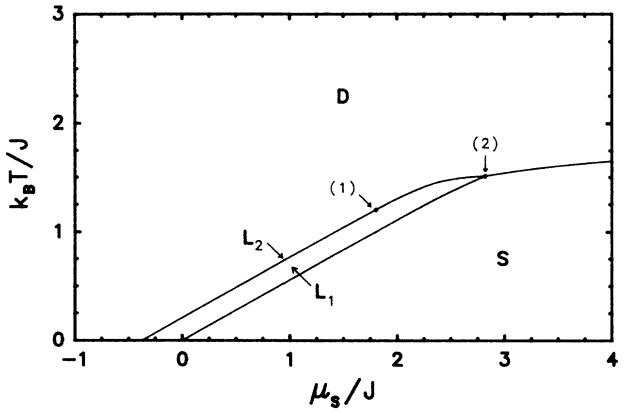

FIG. 9. Same diagram as in Fig. 7, but obtained by the Bethe approximation.

The width, along the μ_s axis in the phase diagram, of the L_1 phase for the water and surfactant mixture is found by subtracting Eqs. (30) and (31),

$$\Delta_{L_1} \simeq -\tfrac{3}{2}(J_1+K_1)-3(J_2+K_2)-\tfrac{3}{2}(J_3+K_3)\ . \qquad (32)$$

This width of L_1 for the binary mixture is three-quarters the width of the similar lamellar phase for the ternary mixture of water, oil, and surfactant. More importantly, this width is positive if and only if the similar width of the ternary mixture is positive. This means that the condition required for the existence of a lamellar phase is the same for both mixtures.

In passing, let us note that the extreme narrowness of the L_2 region in the chemical-potential phase diagram, and the absence of the lamellar phases L_n for $n>2$ at nonzero temperatures disagrees with speculations made by Dawson and Kurtovic.[14] However, the coexistence of water-rich and surfactant-rich uniform phases speculated by Dawson and Kurtovic, replacing our single D phase, can be exhibited by our model with the proper choice of bonding energies.[24] The similarities between the present

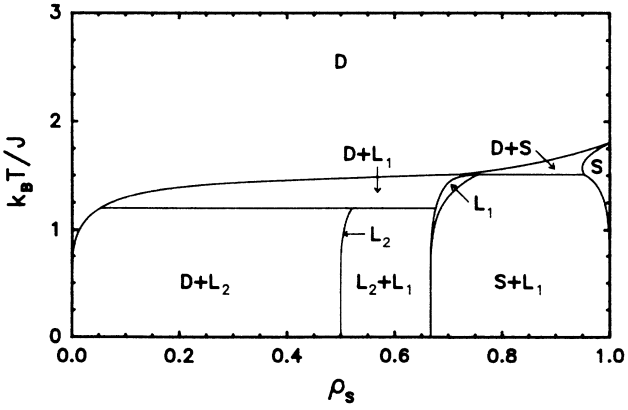

FIG. 10. Same diagram as in Fig. 8, but obtained by the Bethe approximation.

TABLE IV. Coordinates of three points along the phase boundaries in the phase diagram for the binary mixture.

	Mean-field approximation		Bethe approximation	
Point	μ_s/J	k_BT/J	μ_s/J	k_BT/J
1	2.5033	1.5612	1.7997	1.2019
2	3.4164	1.7986	2.8191	1.5109
3	$+\infty$		2.1667 $+\infty$	1.8073

model and the Dawson-Kurtovic model lead us to expect that the latter will exhibit similar behavior to that found here.

VII. DISCUSSION

The existence of lamellar phases in the water-oil-surfactant mixture agrees with experiment. An interesting feature of the present model is the existence of long-period lamellar phases. Although one may not consider the L_2 phase to have a "long" period, it is possible to obtain phases with longer periods by simply adjusting the J_α's and K_α's.[21] Long-period layered phases have been obtained with the model of Widom and co-workers[9,10] and with the spin-1 model of a microemulsion of Schick and Shih.[6] The notable feature of the present model is that these phases are obtained with only NN interactions. This suggests that short-range forces may be one of the mechanisms that produce long-period lamellar phases. Other mechanisms known to do this are long-range electrostatic forces in the case of charged surfactant layers, and fluctuations in the case of flexible surfactant layers.[1,17]

In the phase diagrams plotted in terms of surfactant density, one can observe coexistence regions for the two lamellar phases L_1+L_2. The occurrence of such a region is a consequence of the lattice model. The analogous region for a similar continuous model would presumably be a single phase where the surfactant layer separation changed continuously, decreasing as the surfactant concentration increased.

In real water-oil-surfactant mixtures, one also finds hexagonal and cubic phases. These phases are similar to the lamellar phase in that they exhibit a well-defined geometry of water and oil regions separated by surfactant, the notable difference being that they have an increasingly elaborate geometry. There have been attempts to include these phases in lattice theories.[6,13] A problem with doing this is that the lattice does not realistically allow for the continuous bends characterizing the water-oil interfaces and surfactant layers of the hexagonal and cubic phases. It is likely that a proper description of these phases will require, at least, generalizing the present model to allow for continuous surfactant orientations and generalizing the Hamiltonian. Nevertheless, since the hexagonal and cubic phases are similar in nature to the lamellar phases except for their geometry, it is desirable to retain a model which is simplified due to their absence.

In this paper, we chose the parameters K_α in the Hamiltonian [Eq. (1)] to be zero because we considered them

to be less crucial than the J_α's. We suspect that if we used nonzero K_α's, with magnitudes of order J, then the topology of the phase diagrams would not be significantly altered. However, the K_α's do seem to have an important quantitative effect on the phase diagrams. For instance, when we considered reasonable bonding energies for all the 11 distinct bonds (Table II) and found the corresponding J_α's and K_α's,[25] the tricritical point moved to $(k_B T/J, \rho_s) = (2.89, 0.36)$ from the present (1.66,0.60) as calculated by the Bethe approximation. This shift of the tricritical point to lower surfactant concentration suggests that the region of the disordered phase to the right of the disorder line (Figs. 2–5), which we have associated with a microemulsion, could be moved to significantly lower surfactant concentrations, as it should. We hope to consider this further, along with a more in-depth look at the microemulsion region and its surface tensions with the other phases.

Comments made above for the ternary mixtures in general apply to the binary mixtures of water and surfactant. These mixtures exhibit lamellar, hexagonal, and cubic phases similar to those of the ternary mixture. The micellar phase is the analog of the microemulsion. Here, instead of having regions of water an oil in various geometries separated by surfactant monolayers, there are regions of water separated by surfactant bilayers. The bilayers are arranged as to only expose the polar heads of the surfactant molecules. The binary mixture also exhibits an analog to the disorder line.[26] In fact, the equation of this line is identical to that for the ternary mixture [Eq. (26)] when using the mean-field approximation. We speculate that this line may be related to the experimentally observed critical micelle concentration (CMC) line.[27] We also note, however, that the present model does not produce a lower critical point, which is found experimentally for mixtures of water and nonionic surfactants.[27]

The results for the water-surfactant mixtures were obtained by restricting the σ_i's to 0 and 1. Similar results could also be obtained for oil-surfactant mixtures by restricting the σ_i's to 0 and -1. The phase diagrams for these oil-surfactant mixtures would be the same as those for the water-surfactant mixtures, due to the symmetry of the Hamiltonian. The structure of the phases themselves would differ by symmetry. For instance, the lamellar phases would consist of surfactant bilayers, arranged so as to only expose the tails of the surfactant molecules, separated by oil layers. To obtain results for unequal and nonzero concentrations of water and oil, one could include in the Hamiltonian [Eq. (1)] chemical-potential terms for the water and oil molecules.

In summary, the present lattice model exhibits global phase behavior characteristic of both ternary and binary surfactant mixtures. These features depend crucially on the orientational degrees of freedom allowed for the surfactant molecules, which in the most successful of the previous models[8,12] are mimicked by effective many-body interactions. Further studies are in progress to explore several specific applications of this model.

ACKNOWLEDGMENTS

This work has been supported by a grant from the Natural Sciences and Engineering Research Council, Canada.

[1] R. Lipowsky and S. Leibler, Phys. Rev. Lett. **56**, 2541 (1986); S. Leibler and R. Lipowsky, Phys. Rev. B **35**, 7004 (1987); Phys. Rev. Lett. **58**, 1796 (1987).

[2] S. Leibler and D. Andelman, J. Phys. (Paris) **48**, 2013 (1987).

[3] D. Andelman, M. E. Cates, D. Roux, and S. A. Safran, J. Chem. Phys. **87**, 7229 (1987); P. Balbuena, C. Borzi, and B. Widom, Physica **138A**, 55 (1986); R. E. Goldstein and S. Leibler, Phys. Rev. Lett. **61**, 2213 (1988).

[4] K. Chen, C. Ebner, C. Jayaprakash, and R. Pandit, Phys. Rev. A **38**, 6240 (1988).

[5] J. W. Halley and A. J. Kolan, J. Chem. Phys. **88**, 3313 (1988).

[6] M. Schick and W. H. Shih, Phys. Rev. B **34**, 1797 (1986).

[7] M. Schick and W. H. Shih, Phys. Rev. Lett. **59**, 1205 (1987); G. M. Garneiro and M. Schick, J. Chem. Phys. **89**, 4638 (1988).

[8] G. Gompper and M. Schick, Phys. Rev. Lett. **62**, 1647 (1989).

[9] B. Widom, J. Chem. Phys. **84**, 6943 (1986); K. A. Dawson, M. D. Lipkin, and B. Widom, *ibid.* **88**, 5149 (1988).

[10] B. Widom, J. Chem. Phys. **90**, 2437 (1989).

[11] Generalizations of the model considered by Widom and coworkers are described by V. Talanguer, C. Varea, and A. Robledo, Phys. Rev. B **39**, 7039 (1989), and references therein.

[12] G. Gompper and M. Schick, in *Modern Ideas and Problems in Amphiphilic Science,* edited by W. M. Gelbart, D. Roux, and A. Ben-Shaul (Springer-Verlag, Berlin, in press).

[13] A. Ciach, J. S. Høye, and G. Stell, J. Phys. A **21**, L777 (1988); J. Chem. Phys. **90**, 1214 (1989); A. Ciach and J. S. Høye, *ibid.* **90**, 1222 (1989).

[14] K. A. Dawson and Z. Kurtovic (unpublished).

[15] M. M. Telo da Gama and K. E. Gubbins, Mol. Phys. **59**, 227 (1986).

[16] J. R. Gunn and K. A. Dawson (unpublished).

[17] C. R. Safinya *et al.*, Phys. Rev. Lett. **57**, 2718 (1986); C. R. Safinya, E. B. Sirota, D. Roux, and G. S. Smith, *ibid.* **62**, 1134 (1989).

[18] M. Blume, V. J. Emery, and R. B. Griffiths, Phys. Rev. A **4**, 1071 (1971).

[19] R. Kikuchi, Phys. Rev. **88**, 988 (1951); E. Chacón and P. Tarazona, Phys. Rev. B **39**, 7111 (1989).

[20] W. M. Ng and J. H. Barry, Phys. Rev. B **17**, 3675 (1978).

[21] All the lamellar phases L_n for $n=1$ to 4 are exhibited for both the binary and ternary mixtures, if J_3 and J_4 are set to zero and the other bonding energies are unchanged.

[22] M. Teubner and R. Strey, J. Chem. Phys. **87**, 3195 (1987).

[23] J. Stephson, J. Math. Phys. **11**, 420 (1970).

[24] If J_3 and J_4 are set to $\frac{1}{2}J$, for the binary mixtures there occur distinct water-rich and surfactant-rich uniform phases, exhibiting Ising-like coexistence up to a high-temperature critical point.

[25] Choosing some reasonable energies for the 11 bonds in Table II and making the necessary transformations such that three of the energies were zero, we found $J_1 = J$, $J_2 = 1.5J$, $J_3 = 0.9J$, $J_4 = 0.8J_1$, $K_1 = 2.5J$, $K_2 = 3.0J$, $K_3 = 2.6J$, and $K_4 = 0.3J$.

[26] G. Gompper and M. Schick, Chem. Phys. Lett. (to be published).

[27] W. Wenzel, C. Edner, C. Jayaprakash, and R. Pandit, J. Phys. Condens. Matter. **1**, 4245 (1989).